LETTERS
https://doi.org/10.1038/s42255-019-0115-y
nature metabolism

Succinate accumulation drives ischaemia-reperfusion injury during organ transplantation

Jack L. Martin[1,6], Ana S. H. Costa[2,6], Anja V. Gruszczyk[1,3], Timothy E. Beach[1], Fay M. Allen[3], Hiran A. Prag[3], Elizabeth C. Hinchy[3], Krishnaa Mahbubani[1], Mazin Hamed[1], Laura Tronci[2], Efterpi Nikitopoulou[2], Andrew M. James[3], Thomas Krieg[4], Alan J. Robinson[3], Margaret M. Huang[1,3], Stuart T. Caldwell[5], Angela Logan[3], Laura Pala[5], Richard C. Hartley[5], Christian Frezza[2], Kourosh Saeb-Parsy[1,7] and Michael P. Murphy[3,4,7*]

During heart transplantation, storage in cold preservation solution is thought to protect the organ by slowing metabolism, providing osmotic support and minimizing ischaemia–reperfusion (IR) injury following transplantation in the recipient[1,2]. Despite its widespread use, our understanding of the metabolic changes prevented by cold storage and how warm ischaemia leads to damage is surprisingly poor. Here, we compare the metabolic changes during warm ischaemia (WI) and cold ischaemia (CI) in mouse, pig and human hearts. We identify common metabolic alterations during WI and CI, thereby elucidating mechanisms underlying the benefits of CI and how WI causes damage. Succinate accumulation is a major feature within ischaemic hearts across species, and CI slows succinate generation, thereby reducing tissue damage upon reperfusion caused by the production of mitochondrial reactive oxygen species (ROS)[3,4]. Importantly, the inevitable periods of WI during organ procurement lead to the accumulation of damaging levels of succinate during transplantation, despite cooling organs as rapidly as possible. This damage is ameliorated by metabolic inhibitors that prevent succinate accumulation and oxidation. Our findings suggest how WI and CI contribute to transplant outcome and indicate new therapies for improving the quality of transplanted organs.

Hearts are transplanted following donation after brainstem death (DBD), or following donation after circulatory death (DCD)[5–8]. Cooling the heart at the onset of ischaemia remains the mainstay of organ preservation, although emerging technologies allow preservation of some organs under normothermic and/or normoxemic conditions[8,9]. Rapid cooling minimizes periods of WI during transplantation, which causes non-function of the primary graft, delayed or poor initial function of the graft or chronic graft dysfunction[10,11]. Here we investigated the metabolic alterations during WI that contribute to tissue injury upon transplantation and which are prevented by CI.

We examined the metabolic profiles of mouse hearts and sections of pig and human myocardium under conditions that mimic cold organ storage during transplantation (CI; ~2 °C) and compared these results with those from the samples during WI (37 °C) (Fig. 1a) over time. There was a much faster decline in the ATP/ADP ratio during WI than during CI in tissue from all three species (Fig. 1b–d) — this decreased by over 50% during the first 5 min of WI, whereas 5 min of CI had a negligible effect. In the CI heart, contraction ceased within ~1–2 s, but in the WI heart, contraction continued for ~90 s; however, ATP consumption by contraction during WI did not contribute to changes in ATP/ADP because preventing contraction by cardioplegia did not affect the ATP/ADP ratio (Extended Data Fig. 1a). The total amount of ATP and ADP (ΣATP + ADP) was also better maintained during CI than during WI (Fig. 1e–g), whereas AMP accumulation was faster during WI than in CI (Extended Data Fig. 1b). Thus, CI preserves tissue ATP/ADP and slows the loss of adenine nucleotides.

During ischaemia, oxidative phosphorylation stops and glucose is no longer delivered by the blood; hence, the ATP/ADP ratio is sustained by glycogen-fuelled glycolysis[12], generating lactate (Extended Data Fig. 2a). Glycogen in the mouse and pig tissue was more rapidly depleted during WI, but depletion eventually halted under these conditions, despite 20–25 % of the glycogen remaining (Extended Data Fig. 2b,c). During CI, glycogen depletion was slower, but continued until all glycogen was consumed (Extended Data Fig. 2b,c). During WI, lactate initially accumulated but then plateaued, whereas during CI, the rate at which lactate built up was far slower, but continued throughout CI (Extended Data Fig. 2d–h). In the mouse heart, lactate accumulation ceased when glycogen breakdown stopped (dashed red line in Extended Data Fig. 2b,d). The lactate/pyruvate and NADH/NAD^+ ion intensity ratios both increased far more rapidly and extensively during WI than during CI in the mouse heart (Extended Data Fig. 2h,i). Measurement of glycolytic intermediates in the mouse heart showed an accumulation of the GAPDH substrate glyceraldehyde-3-phosphate during WI, but the loss of products downstream of 3-phosphoglycerate kinase, 3-phosphoglycerate and phosphoenolpyruvate, as compared to CI (Extended Data Fig. 3). These two enzymes utilize NAD^+ and ADP, and thus are likely inhibited by an elevated NADH/NAD^+ ratio and depletion of ADP (Extended Data Fig. 2a). This might slow glycolysis during WI, even though glycogen stores remain. Thus, during WI, there was rapid glycogen depletion to drive glycolysis, which was slowed by CI.

[1]Department of Surgery and Cambridge NIHR Biomedical Research Centre, Biomedical Campus, University of Cambridge, Cambridge, UK. [2]MRC Cancer Unit, University of Cambridge, Hutchison/MRC Research Centre, Cambridge, UK. [3]MRC Mitochondrial Biology Unit, University of Cambridge, Cambridge, UK. [4]Department of Medicine, University of Cambridge, Cambridge, UK. [5]School of Chemistry, University of Glasgow, Glasgow, UK. [6]These authors contributed equally: Jack L. Martin, Ana S. H. Costa. [7]These authors jointly supervised this work: Kourosh Saeb-Parsy, Michael P. Murphy.
*e-mail: mpm@mrc-mbu.cam.ac.uk

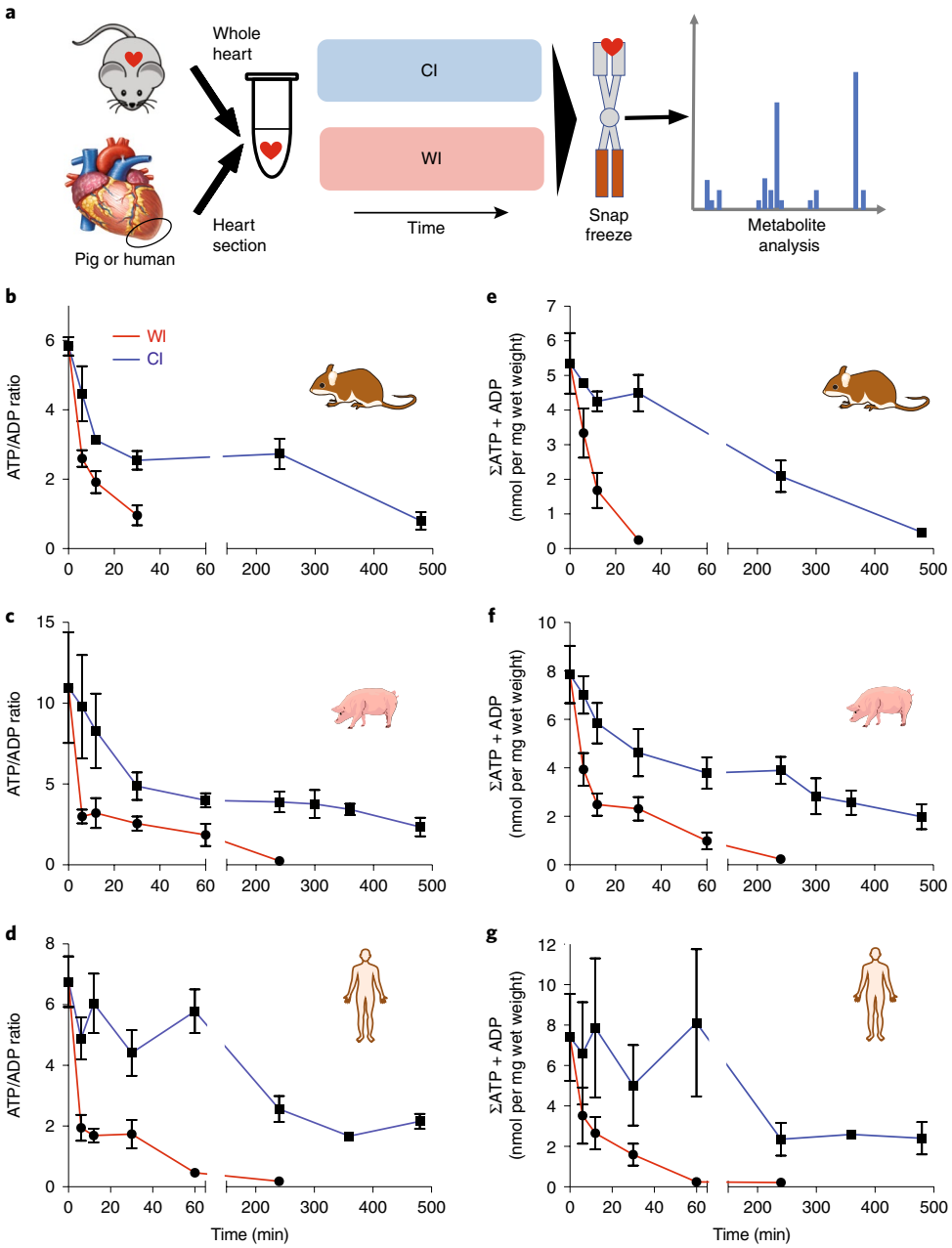


Fig. 1 | The cardiac ATP/ADP ratio during WI and CI. a, A schematic illustrating the experimental design mimicking ischaemia during transplantation. The whole mouse heart (~150–180 mg), or sections from the transected apex of the pig or human heart (~120 mg) were either immediately clamped frozen at liquid nitrogen temperature to generate a baseline sample under fully oxygenated 'normoxic' conditions, or were incubated to induce WI (37 °C) or CI (~2 °C) for the indicated times prior to freeze clamping. Tissues were then extracted and metabolites assayed. ATP and ADP were determined in heart tissue after various times of WI or CI. **b**–**d**, The ATP/ADP ratio for (**b**) mouse, (**c**) pig and (**d**) human. **e**–**g**, The sum of ATP and ADP (nmol mg^{-1} wet weight) for (**e**) mouse, (**f**) pig and (**g**) human. Data are means ± s.e.m., $n = 5$ (pig), 4 (human). For **b** and **e**, data are means ± s.e.m., WI 6 and CI 240 min, $n = 11$; WI 0, 12, 30 and CI 0 min, $n = 9$; CI 6 min, $n = 7$; CI 12 min, $n = 4$; CI 30 min, $n = 3$.

To assess ischaemic metabolism more broadly, we performed a liquid chromatography–mass spectrometry (LC–MS)-based metabolomics analysis of mouse, pig and human heart tissue at various times under CI and under WI (Supplementary Data 1a–c). Fifty-four metabolites were detected ubiquitously at up to 30 min WI and 480 min CI, and changes in their abundances are presented as a heat map, which reveals similar overall profiles in mouse, pig and human heart tissue (Extended Data Fig. 4). We expanded the metabolome coverage to 107 metabolites for the mouse samples that underwent a second LC–MS analysis, which generated an extended heat map (Extended Data Fig. 5).

To compare how these metabolites changed between WI and CI (Supplementary Data 2) we generated volcano plots for mouse, pig and human heart tissue (Fig. 2a–c). Strikingly, most of the significant metabolic changes between WI and CI at the 30-min time point were comparable between mouse, pig and human hearts (red and green symbols). The only metabolites that changed in qualitatively different ways between species were fumarate and malate (Supplementary Data 1), which both accumulated during WI in the pig tissue, but decreased in the mouse and showed minor changes in the human. As can be seen, there were notable and similar changes in many metabolites for all three species, including in choline,

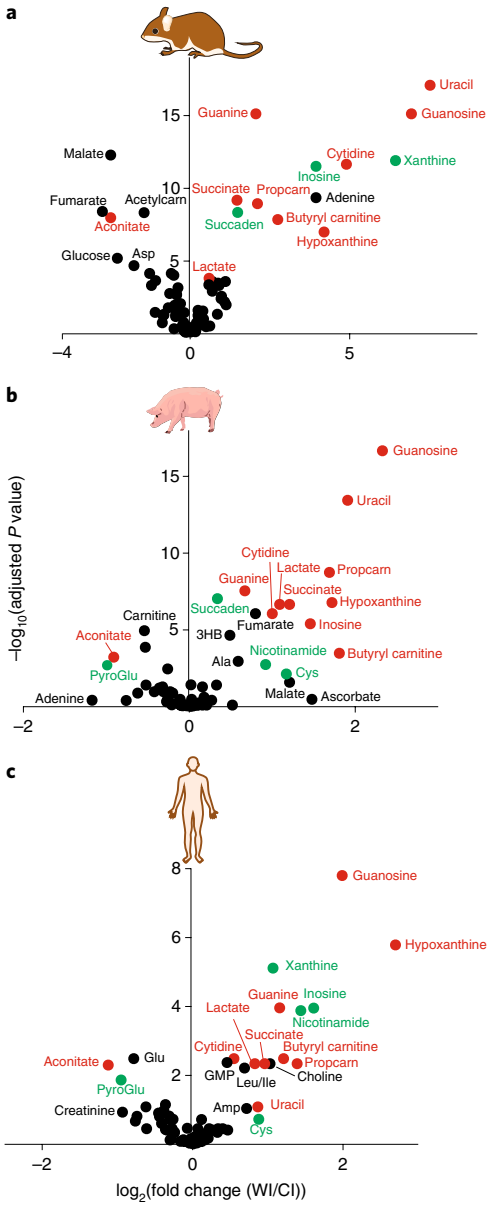


Fig. 2 | Volcano plots of metabolites that are significantly different between 30 min WI and 30 min CI. Volcano plots showing $-\log_{10}$ of the adjusted *P* value plotted against the $\log_2$ of the fold-change in metabolite abundance between 30 min WI and 30 min CI for (**a**) mouse ($n=5$), (**b**) pig ($n=5$) and (**c**) human ($n=4$). Fold-changes and *P* values between time points were calculated by using linear modelling with an empirical Bayes approach as implemented in the 'limma' package of R. We adjusted for multiple-testing using the Benjamini–Hochberg procedure. Metabolites that changed in the same way in all three species are in red. Metabolites that changed in the same way in two of the species but were not detected, or did not change markedly, in the third are in green. All other metabolites are in black. Proprionylcarnitine, propcarn; acetyl carnitine, acetylcarn; succinyl adenosine, succaden; 3-hydroxybutyrate, 3HB; pyroglutamic acid, pyroGlu.

nicotinamide, alanine, proline, aconitate and branched chain amino acids, and in the breakdown products of purines and pyrimidines.

Succinate increased dramatically during WI in all species (Fig. 2a–c). This finding was of particular interest because succinate accumulation during ischaemia contributes to IR injury upon reperfusion via generation of ROS by reverse electron transport (RET) at mitochondrial complex I (refs. [3,4]). Quantification of succinate levels over time showed that during WI, there was rapid succinate accumulation within 6 min that increased further and plateaued at about 30 min (Fig. 3a–c). During CI, succinate accumulation was far less, and even after 4 h of CI—the traditional storage limit for human hearts to be viable for transplantation—the succinate level was less than that after 6 min of WI (Fig. 3a–c). Even after extending CI of mouse hearts to 12 h, the succinate level was still similar to that after 12 min of WI (Fig. 3d). The relative changes (Fig. 3a–c) as well as the absolute succinate levels (Fig. 3e) were remarkably similar in mouse, pig and human heart tissue. Cardioplegia slightly decreased succinate levels during WI in the mouse hearts (Extended Data Fig. 6a), but even so, the relative accumulation was still 4- to 5-fold above the levels during CI, suggesting that succinate accumulation is unrelated to changes in muscle contraction. Considering that succinate accumulation is driven by the interconversion of fumarate and succinate by succinate dehydrogenase (SDH), we next assessed the succinate/fumarate ion intensity ratio (Fig. 3f–h). This showed a major increase during WI in mouse tissue, with a less pronounced increase in that from pig and human; that in all cases, this was slowed by CI. We conclude that there is a dramatic accumulation of succinate during WI in mouse, pig and human hearts that is greatly slowed by cooling.

Succinate accumulation in ischaemic mouse hearts was proportional to temperature (Extended Data Fig. 6b). When a mouse heart was transferred to cold static storage, its temperature dropped to ~2 °C within 1 min (Extended Data Fig. 6c), likely minimizing succinate accumulation. However, the much larger human heart (~300 g versus ~150 mg for the mouse) would take far longer to cool during transplantation, potentially leading to succinate accumulation due to WI. To assess this, we measured the core and the surface temperatures of a pig heart (~300 g) during its flushing with cold preservation solution via the aortic root cannula immediately after cross clamp in conjunction with topical application of a crushed ice/cold saline mix (Fig. 4a), as occurs during human heart transplantation. The core took ~15 min to reach 4 °C, despite our use of the same rapid cooling procedures used during clinical heart transplantation. This slow cooling led to significant succinate accumulation (Fig. 4b). Therefore, the inevitable periods of WI during organ retrieval, cooling and storage during transplantation will lead to considerable succinate accumulation.

Measuring mouse heart temperature during retrieval for transplantation indicated that after the blood supply was stopped, the organ cooled slowly while the vessels were being prepared for transplantation, despite frequent topical application of cold saline (Extended Data Fig. 6d). This period of ischaemia as the organ cooled led to succinate accumulation that was retained during subsequent cold storage (Extended Data Fig. 6e). To determine whether the accumulated succinate could contribute to tissue damage by driving IR injury upon reperfusion during transplantation, we used a mouse model of syngeneic transplantation, in which a heart is transplanted heterotopically into the abdomen[13,14]. During transplantation, there is a further period of ~20 min ischaemia as the heart is anastomosed to the blood vessels in the recipient mouse. During this time, the heart gradually warmed up, despite cooling by topical saline, leading to a further accumulation of succinate (Fig. 4c). Within 5 min of reperfusion following transplantation, the succinate level returned to baseline (Fig. 4c). Therefore, during retrieval, storage and transplantation, donor hearts accumulate succinate that is rapidly oxidized upon reperfusion in the recipient.

To model the slower cooling of a human heart during retrieval, we next assessed whether increasing the duration of WI (in addition to the ~8 min during retrieval and the ~20 min during anastomosis in the recipient) contributed to damage upon transplantation (Fig. 4d). Hearts did not survive transplantation when exposed to more than ~12 min WI after retrieval. Hearts transplanted after a further 12 min WI had increased damage, as evaluated 24 h after

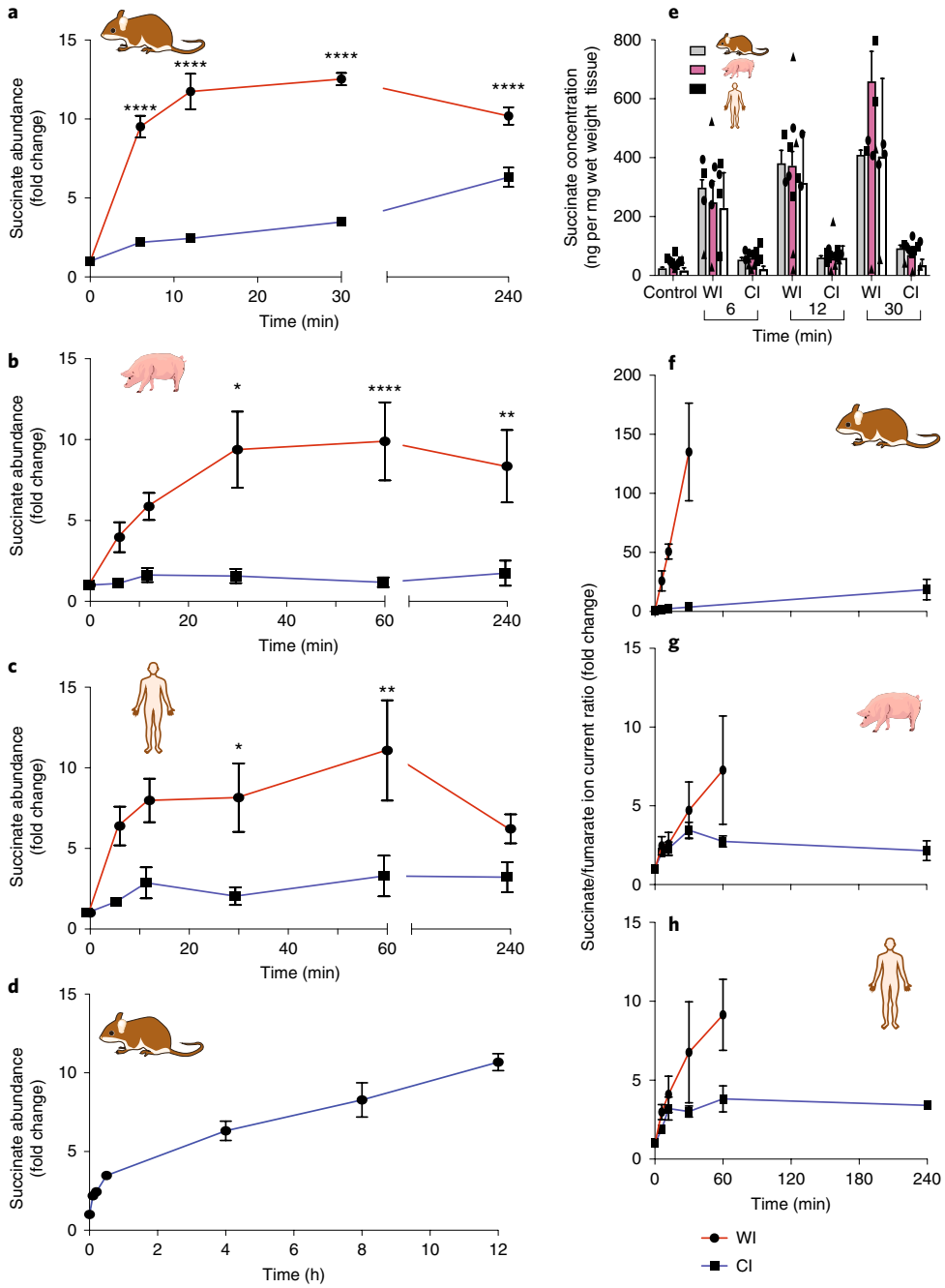


Fig. 3 | Succinate levels in the heart during WI and CI. a–d, Fold change in succinate abundance under WI or CI, relative to normoxic heart tissue in mouse (**a**,**d**, $n=6$), **b** pig (**b**, $n=4$) and human (**c**, $n=4$). Data are means ± s.e.m. For **a**–**c**, the significant difference between groups were measured by two-way ANOVA, with multiple comparisons at individual points by Sidak test (*$P<0.05$, **$P<0.01$, ****$P<0.0001$). **e**, Absolute succinate concentrations for conditions described in **a**–**d**. Data are means ± s.e.m. Mouse ($n=6$), pig ($n=4$) and human ($n=4$). **f**–**h**, Relative change in succinate/fumarate ratio under WI or CI, compared to normoxic heart tissue. Data are means ± s.e.m. Mouse ($n=6$), pig ($n=4$) and human ($n=4$). These data are presented as relative changes in the ratio of the ion current for these metabolites, which is proportional to, but not the same as, the true ratio of the metabolite levels.

transplantation by release of troponin (Fig. 4e) and mitochondrial DNA (mtDNA) from damaged tissue[15,16] (Fig. 4f,g) and by damage to mtDNA within the tissue (Fig. 4h). As the extra period of WI will increase succinate levels (Fig. 4c), these findings are consistent with increased WI contributing to heart damage through elevated succinate driving mitochondrial ROS production upon reperfusion. However, many other factors might contribute to tissue damage in addition to succinate. Therefore, we next explored the role of succinate accumulation alone in the absence of other confounding factors associated with WI.

To assess the role of succinate accumulation in heart damage upon transplantation, independent of other effects of WI, we increased heart succinate levels by infusing *bis*-acetoxymethyl succinate (AMS) into the mouse organ[17]. AMS generates succinate within cells that can then be oxidized by SDH[17]. Hearts were infused with AMS and incubated at 4 °C for 30 min and then 20 min at 37 °C to mimic the CI and anastomosis periods experienced in the heterotopic transplant model. The tissue succinate concentration increased little during CI but significantly increased during subsequent simulated anastomosis as a result of enhanced tissue esterase

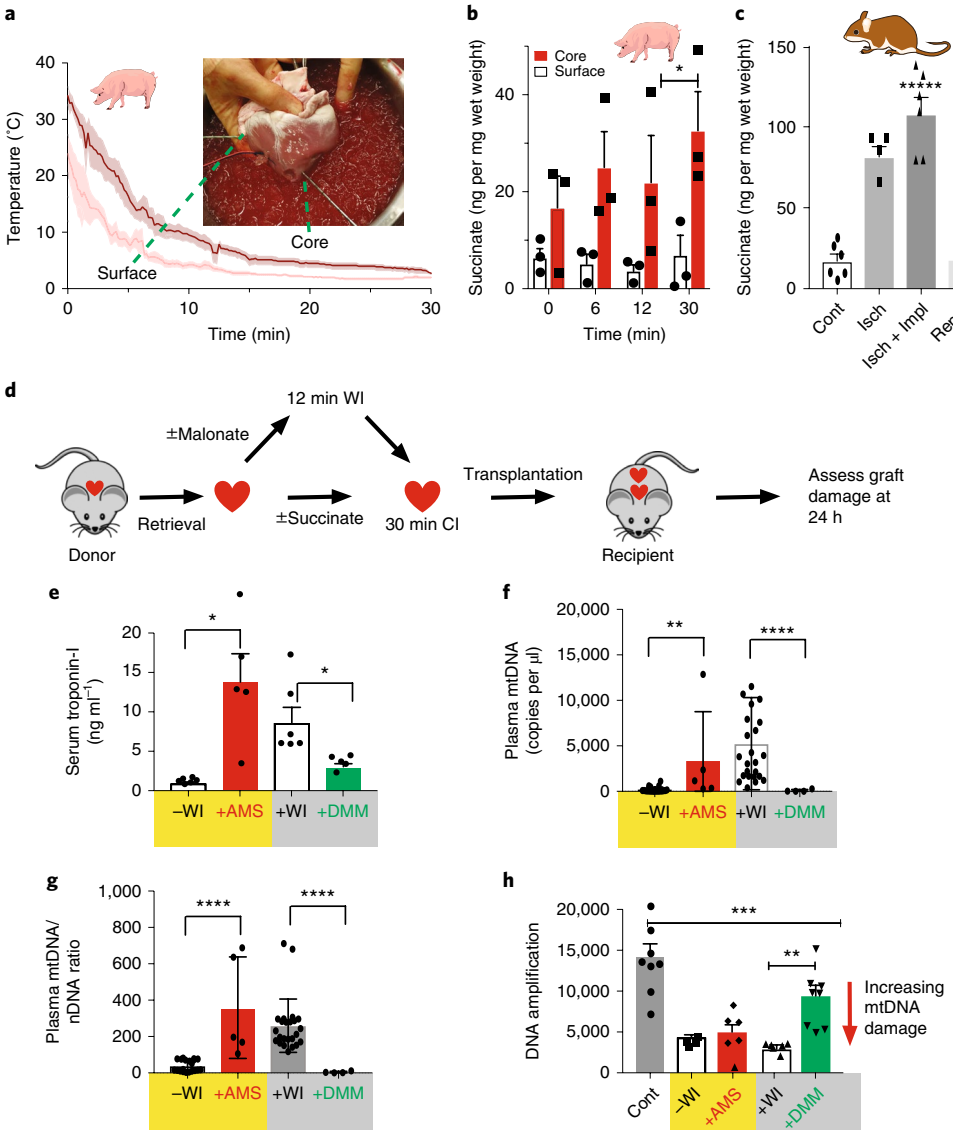


Fig. 4 | Preventing pathological consequences of succinate metabolism during heart transplantation. a, Surface and core temperature of pig heart during flush with cold University of Wisconsin (UW) solution. Following retrieval, the heart was flushed with cold solution and immersed in slushed ice. The mean temperature ($n=4$) every 10 s is shown ± s.e.m. (shaded). The inset shows the temperature probes. **b**, Surface and core succinate of the pig heart, treated as described in **a**. Core and surface tissue biopsies were taken at 0, 6, 12 and 30 min and frozen, and succinate concentration was then measured ($n=3$, data are means ± s.e.m.). *$P<0.05$, by a two-way ANOVA with Sidak's multiple-comparison test. **c**, Succinate concentration in the mouse heart after standard retrieval and 30 min CIT (Isch), after standard retrieval and 30 min CIT and anastomosis (Isch. + Impl), and finally after 5 min reperfusion ('Reper.'). Data mean ± s.e.m. (Cont and Isch + Impl, n = 6; Isch, n = 4; Reper, n = 3). Compared to control (Cont.) by one-way ANOVA with Bonferroni multiple comparisons tests (***P < 0.001, ****P < 0.0001). **d**, Schematic of heterotopic heart transplantation in mice, with a further 12 min WI after retrieval, followed by 30 min cold storage. **e**–**g**, Hearts were infused with DMM (3.4 mg) or saline prior to cardioplegia and then exposed to 12 min WI, and then stored cold for 30 min, or infused with cardioplegia solution ± AMS (3.2 mg), followed by cold storage for 30 min. All hearts were then transplanted into recipients and 24 h later serum troponin (**e**), mtDNA (**f**) or mtDNA/nuclear DNA ratio (**g**) were measured. **h**, mtDNA damage in the donor heart was measured at 24 h after transplantation using a PCR assay. The greater the ratio of amplification, the less damage to the mtDNA. **e**–**g** (–WI, $n=20$; +AMS, $n=5$; +WI, $n=24$; +DMM, $n=4$); **h** (Cont, $n=8$; –WI, $n=4$; +AMS, $n=5$; +WI, $n=7$; +DMM, $n=8$). Data are means ± s.e.m. *$P<0.05$, **$P<0.01$, ****$P<0.0001$ by one-sided unpaired Student's t-test with Welch's correction.

activity and AMS hydrolysis at 37 °C compared to 4 °C (Extended Data Fig. 6f). AMS-treated hearts exhibited increase damage upon transplantation, as measured 24 h later by the release of troponin (Fig. 4e) and mtDNA (Fig. 4f,g) and by damage to mtDNA within the transplanted heart (Fig. 4h). Infusion of the same amount of *bis*-acetoxymethyl fumarate, which readily delivers fumarate within cells (Extended Data Fig. 6g), did not lead to damage (Extended Data Fig. 6h,i), indicating that disruption to cardiac damage is specific to succinate over other tricarboxylic acid (TCA) cycle intermediates. These findings show that succinate alone is sufficient to cause extensive damage to the transplanted heart. This is consistent with succinate accumulation being responsible for at least part of the increased heart damage caused by an additional 12 min of WI.

Finally, to determine whether this increased heart damage due to 12-min-further WI was decreased by inhibiting succinate accumulation and oxidation, we infused dimethyl malonate (DMM)

prior to initiating retrieval and cold storage to load the heart with malonate (Fig. 4d and Extended Data Fig. 6j). Hydrolysis of DMM will generate the SDH inhibitor malonate within the tissues, slowing both the accumulation of succinate during ischaemia (Extended Data Fig. 6k) and its oxidation upon reperfusion and thereby protecting against IR injury[4,18,19]. DMM protected the heart against damage as measured 24 h after transplantation (Fig. 4e–h). Thus, succinate accumulation during WI and its oxidation upon reperfusion are significant contributors to IR injury in transplantation, and amelioration of these decreases organ injury.

We can draw a number of noteworthy conclusions from our assessment of metabolic changes during WI and CI in mouse, pig, and human heart samples. First, metabolism during WI and CI was comparable between mouse, pig and human hearts, encouraging the development of therapies using animal models. Second, during WI, there was a dramatic decrease in the ATP/ADP ratio that is slowed by CI. The fall in ATP/ADP ratio during WI was paralleled by the generation of AMP via adenylate kinase, leading to AMP breakdown and an accumulation of products from purine and pyrimidine breakdown. Therefore, a major benefit of CI is preserving the ATP/ADP ratio and preventing loss of adenine nucleotides, the loss of which likely contributes to increased RET at reperfusion[20]. Third, there was a rapid decrease in glycogen with WI and an associated increase in lactate, consistent with anaerobic glycolysis driving ATP production. This loss of glycogen and production of lactate was far faster in WI than in CI, but there was incomplete breakdown of glycogen in WI, suggesting that the rising NADH/NAD^+ ratio and/or the falling ADP level slowed glycolysis and glycogenolysis. Finally, succinate accumulated very rapidly in all species during WI. Ischaemic succinate accumulation most likely arises as a consequence of the build-up of NADH and other metabolites contributing to succinate generation by reversal of SDH[3,4]. However, further work will be required to assess whether glutaminolysis also contributes to succinate accumulation during WI, as recently proposed[21]. This selective accumulation of succinate instead of other TCA metabolites during ischaemia might be the consequence of multiple metabolic reactions that converge on succinate, which cannot be metabolized further under these conditions, in contrast to other TCA metabolites.

Importantly, succinate accumulation occurred when we simulated donation after brain stem death (DBD) in which normoxaemic organs are cooled in situ immediately after cessation of circulation and are therefore often considered to be exposed to only CI. However, these organs are exposed to at least a few minutes of WI as the organs become ischaemic and cooling commences, but before the organ reaches ~2 °C. Thus, damage caused by WI is an inevitable, albeit not widely recognized, part of all transplantation despite the widespread reliance on cold flush and storage to enhance organ preservation.

In summary, in the first application of detailed and time-resolved metabolomics to transplant surgery to our knowledge, we have shown that succinate accumulation is an important but underappreciated cause of pathology during organ transplantation. We propose that preventing the accumulation and oxidation of succinate during transplantation with new therapies and changes in methodology to ensure more rapid cooling will improve outcomes of transplantation.

Methods

Materials. The composition of UW storage solution used is (in mM): potassium lactobionate, 50; KH_2PO_4, 25; $MgSO_4$, 5; raffinose, 30; adenosine, 5; glutathione, 3; allopurinol, 1; and hydroxyethyl starch (50 g L^{-1}). The composition of St. Thomas' cardioplegia solution is: (NaCl 110.0 mM, $NaHCO_3$ 10.0 mM, KCl 16.0 mM, $MgCl_2$ 16.0 mM, $CaCl_2$ 1.2 mM, pH 7.8). Dimethyl malonate was from Thermo Fisher Scientific, UK. Tissue samples were incubated in polypropylene tubes, either 1.5 ml (Ref no. 72.690.001) or 50 ml (Ref no, 62.547.004), both from Sarstedt, Nümbrecht, Germany.

Animals. Female mice (C57BL/6J (B6/J)) aged 10–20 weeks and weighing 16–22 g were purchased from Charles River Laboratories, UK. Mice were maintained in specific-pathogen-free animal facilities with ad libitum access to food and water. Mice were picked at random from the same cage and assigned to control and experimental arms, but no effort was made to ensure that littermates were used as the controls. Large white male (Landrace) pigs (45–55 kg) were supplied by Envigo and were acclimated for a minimum of 7 d prior to experiments, with ad libitum access to food and water. All animal experiments were approved by the UK Home Office under the Animals (Scientific Procedures) Act 1986. Mouse experiments were covered by PPL 80/2638.

Human tissue. Heart biopsies were taken from deceased human DBD donors deemed unsuitable for cardiac transplantation aged 36–69 (Supplementary Table 1). Informed consent for the use of the human tissue for this project was provided by the donors' families. Ethical approval for the studies was obtained from NRES Committee East of England—Cambridge South (REC Reference 15/EE/0152).

Mouse heart experiments. C57BL/6 mice (female) were anaesthetized with isoflurane (Abbott Laboratories, US) 2 MAC and O_2 at 2 L min^{-1}. Heparin (100 µL bolus (25 iU) Leo Pharma A/S, Ballerup, Denmark) was administered intravenously into the inferior vena cava (IVC) prior to retrieval. Hearts were excised by division of the major vessels. To measure metabolite concentrations in the heart under baseline conditions in vivo, the still-beating heart of an anesthetized mouse was rapidly frozen using Wollenberg clamps at liquid nitrogen (LN_2) temperature, taking ≤5 s to become frozen. For CI, the heart was placed directly in UW solution at ~2 °C. Under these conditions, the ventricles pulsed once or twice before stopping. For WI, the excised heart was left in the abdomen of the animal, with the abdominal wound closed and the animal maintained on a 37-°C heating pad with a relayed rectal temperature probe. For analysis at various times the whole heart was clamped at LN_2 temperature as above. At various times the tissues were rapidly snap-frozen and stored at −80 °C until analysis. Fully oxygenated 'normoxic' heart tissue, snap-frozen immediately upon cessation of circulation, was used as control. Tissues were stored at −80 °C until extraction and analysis.

To replicate heart retrieval with retrograde flushing of the coronary vessels during retrieval (Extended Data Fig. 4e), the donor animal was prepared as described above. Following exsanguination, the great vessels were prepared for implantation[22]. The thoracic cavity was entered by dividing the diaphragm and adequate exposure achieved by dividing the ribs laterally up to the thoracic inlet and retracting the anterior rib cage cranially. The IVC or caudal caval vein, left SVC or cranial caval vein and right SVC or cranial caval vein were ligated with silk ties. The fat and connective tissue was dissected between the aorta and pulmonary artery prior to division of the ascending aorta at the level of the innominate artery. If the heart were to be flushed, the innominate, right carotid and right brachiocephalic artery were ligated and divided. The descending aorta was then divided. The left and right pulmonary arteries were divided adjacent to their bifurcation, and the connecting vessel wall was divided to create a single opening. During dissection and ligation of vessels, the heart was topically cooled intermittently with 0.9% wt/vol sodium chloride, kept on ice. Following ligation of the pulmonary artery, blood remaining in the ventricles was squeezed out. The pulmonary veins were ligated en masse, and the heart was excised. 500 µL Soltran (Baxter Healthcare) was then injected via a fine bore (0.28 × 0.165 mm) polyethene tube (Portex tubing, Smith Medical International Ltd, UK) into the aorta to antegrade flush the coronary arteries. The prepared hearts were then placed in UW solution at ~2 °C for various durations of CI, after which the whole heart was clamped at the LN_2 temperature as described above. For other mouse-heart experiments, a 500 µL bolus of St Thomas' Cardioplegia solution was administered by IVC injection. Complete cessation of heart beat was observed visually within 2 s. Dimethyl malonate (DMM) was administered as an infusion over 10 min via the IVC by a microinfusion pump (Kd Scientific, Holliston, MA, USA) using a fine bore (0.28 × 0.165 mm) polyethene tube (Portex tubing, Smith Medical International Ltd, UK) prior to the administration of cardioplegia. Control animals were infused with 0.9% wt/vol sodium chloride by microinfusion pump (Kd Scientific, Holliston, MA, USA). Bis(acetoxymethyl)succinate (with 5% DMSO) or bis(acetoxymethyl)fumarate (with 30% DMSO) was administered in the cardioplegia solution. Hearts from donor mice were transplanted heterotopically into a syngeneic recipient[13,14]. The donor heart was transplanted heterotopically into the abdomen of the recipient animal using a microsurgical technique. The recipient mouse was weighed before being anaesthetized with isoflurane (Abbott Laboratories, US) and oxygen at 2 L min^{-1}. The skin at the operative site was shaved and prepped with chlorhexidine gluconate (4% wt/vol). Analgesia was administered by subcutaneous injection of 100 µl Temgesic (Indivior, UK) diluted in 500 µl 0.9% wt/vol sodium chloride to the nape of the animal. The animal was transferred to the operating table and secured in a supine position using adhesive tape, and the animal's rectal temperature was measured continuously using a rectal thermometer. It was maintained at 37 °C ± 1 °C using a relayed variable heat mat. A midline laparotomy was performed, and abdominal exposure was achieved using a self-retaining retractor. The bladder was emptied by gentle pressure using sterile cotton buds. The small bowel and colon were deflected superiorly, and a small strip of connective tissue divided to facilitate this maneuver. The abdominal viscera were

retracted and covered with moistened sterile gauze to provide adequate exposure to the abdominal aorta and IVC, and adequate moisture was maintained throughout the procedure by periodic topical irrigation. The connective tissue overlying the abdominal aorta and IVC was divided by a combination of sharp and blunt dissection. The posterior lumbar vessels were identified and ligated using 7-0 silk ties. Non-crushing vascular clamps were applied to the vessels distal to the renal vessels and proximal to their bifurcation. The IVC was emptied via a venotomy created with a 31-gauge needle. An arteriotomy was then made in the aorta, and this was extended using micro-surgical scissors to match the diameter of the donor aorta. The lumen was flushed with 0.9% wt/vol sodium chloride to remove any remaining blood and clots. The donor heart was then retrieved from cold storage and placed into the right side of the recipient's abdomen with the remnant ascending aorta adjacent to the arteriotomy. A small piece of gauze moistened with cold (1–2 °C) 0.9% wt/vol sodium chloride was placed over the heart to minimize warming. Periodic topical application of (1–2 °C) 0.9% wt/vol sodium chloride occurred on the donor heart during the procedure. Cranial and caudal stay sutures were placed between the donor and recipient vessels using 10-0 nylon Bear surgical suture on a round-bodied 4-mm (3/8) needle (Bear Medic Corp., Tokyo, Japan). A continuous end-to-side anastomosis run in a counter-clockwise direction was then constructed from the caudal stay suture. After completing one side of the anastomosis, the heart was turned to the animal's left side to enable access and completion of the anastomosis. The venotomy on the IVC was then extended in a cranial direction. The pulmonary artery was anastomosed in a similar fashion using 10-0 nylon Bear surgical suture. Over tightening of sutures was minimized to ensure there was no constriction of the anastomosis. Cut pieces of Surgicel (Ethicon, Johnson and Johnson, US) were applied around the anastomosis. The distal clamp was removed followed by the proximal clamp. Satisfactory perfusion was indicated by a bright red heart displaying strong rhythmic contractions, and warmed, topical 0.9% wt/vol sodium chloride was applied to the heart to expedite this process. The abdominal fascia and skin were closed in two layers with continuous 5-0 vicryl (Ethicon, Johnson and Johnson, UK). Following reperfusion and closure of the midline wound 500 µl of 0.9% sterile saline was injected subcutaneously. Animals were recovered in an incubator at 28 °C overnight on soft, dry bedding with food and water. Animals that developed post-operative hind-limb paralysis were killed immediately. The next day, animals were returned to standard cages with standard rodent diets. All transplanted hearts contracted spontaneously following reperfusion. Hearts were excised by division of the anastomosed vessels at chosen time points after reperfusion, and the hearts were snap frozen using a Wollenberg clamp and stored at −80 °C until tissue extraction. Animals were randomly allocated to control and treatment groups and the analysis was performed blinded to the experimental groups.

Pig heart experiments. Pigs were pre-medicated with intramuscular ketamine (10 mg.per kg (body weight)), medetomidine (0.02 mg. per kg (body weight)) and midazolam (0.1 mg. per kg (body weight)). A peripheral intravenous catheter was placed in the marginal ear vein, and Propofol was used as anaesthesia. Pigs were intubated and pure oxygen was supplied with intermittent positive pressure ventilation in order to maintain normocapnia. Anaesthesia was maintained with continuous infusions of propofol (starting at 10 mg. per kg (body weight) per hour[1] and titrating down to effect) and either remifentanil (starting at 2.4 µg per kg (body weight) per hour and titrating up to effect) or alfentanil (starting at 30 µg per kg (body weight) per hour and titrating up to effect). If required, isoflurane was provided at approximately 2% to maintain anaesthesia. Saline was administered intravenously at approximately 10 ml per kg (body weight) per hour. During anaesthesia a Datex Ohmeda Cardiocap patient monitoring system was used to monitor ECG waveform, pulse oximetry, temperature and capnography parameters. Immediately following euthanization (induced rapidly with an overdose of approximately 200 mg per kg (body weight) pentobarbitone), the thoracic cavity was accessed through the diaphragm and the apex of the heart (~20–30 g) was amputated with a scalpel under terminal anaesthesia. We note that this retrieval procedure, particularly the use of anaesthesia, is unavoidable, but is slightly different from that used in human transplantation. A full thickness tissue sample (~120 mg) was immediately clamped frozen using Wollenberger clamps at LN_2 temperature, which took ≤5 s from cessation of aortic pulse to freezing. The rest of the tissue was cut in half, with 1 half transferred to cold storage solution and then further cut into smaller pieces (~120 mg), which were stored in UW storage solution at ~2 °C. The other half of the heart tissue was also cut into sections (~120 mg), which were stored in a humidified atmosphere at 37 °C by suspension above saline in sealed Eppendorf tubes. At various times, the tissues were then frozen using Wollenberger clamps at LN_2 temperature and stored at −80 °C until analysis.

To measure the core and surface temperature and tissue succinate of the porcine heart following rapid retrieval and back-table flush, the pig was anaesthetized and euthanized as described above. After circulatory arrest was confirmed, the thoracic cavity was then rapidly accessed through an incision in the diaphragm, and heart was rapidly retrieved by division of the great vessels. On removal from the thoracic cavity, a 'time-zero' surface wedge and core needle biopsy were immediately taken and clamp frozen in LN_2. The core and surface temperature probes (K-type thermocouple, Hanna Instruments, Bedfordshire) were then inserted into the heart. The core temperature probe was inserted into the septum using a hollow biopsy needle. A small incision was made in the surface of the right ventricle, in which the surface probe was inserted and sutured in place. This step took between 1-2 minutes to complete. Temperature recording then commenced, and the heart was submerged in a pre-prepared dish of slushed ice and UW solution. The temperature was recorded every second by a digital data-logger connected to the temperature probe (EL-USB-2 LC, Lascar Electronics, Wiltshire). A 14-G French cannula was used to flush the coronary circulation with cold UW solution. A third temperature probe was used to measure the temperature of the solution as it entered the heart. The coronary sinuses at the base of the aorta were alternately cannulated, and effective flushing of the circulation could be directly observed by flushing of blood with preservation solution in the surface coronary vessels. The time taken to flush the heart with 500 ml cold UW solution was recorded in each case. Further surface wedge and core-needle biopsies were taken at 6, 12 and 30 min.

Human heart experiments. Human donation after brainstem death (DBD) donors undergoing abdominal multiorgan retrieval but for whom cardiothoracic organs had been declined for transplantation were identified (Supplementary Table 1). Formal consent for research was obtained from the families of the donors. A thoracotomy was performed as a routine part of the abdominal organ retrieval procedure, thus allowing a sample (~20–30 g) of myocardium from the apex of the still-beating heart to be removed at the same time as exsanguination and cross clamp of the donor during organ retrieval. The heart tissue was frozen in Wollenberg clamps, taking <5s to go from the beating oxygenated heart to frozen sample. After this base line sample, further samples (~120 mg) were removed, maintained at either 37 °C or ~2 °C as described for the pig tissue, and at various times frozen and stored at −80 °C.

Tissue extraction and metabolite analysis by LC–MS. Frozen tissue samples were weighed into Precellys tubes prefilled with ceramic beads (Stretton Scientific Ltd., Derbyshire, UK), and an exact volume of extraction solution (50% methanol, 30% acetonitrile and 20% water) was added to obtain 40 mg specimen per ml of extraction solution, thus allowing for comparisons between experimental conditions for the same metabolite. Samples were lysed using a Precellys 24 tissue homogenizer (Bertin Corp, Rockville, MD 20850, USA. 5500 r.p.m. 15 seconds × 2) and then centrifuged (16,162 × g for 10 min at 4 °C). The supernatant was transferred to glass vials (Microsolv Technology Corp., Leland, NC 28451, USA) and stored at −80 °C until LC–MS analysis.

LC–MS analyses were performed on a Q Exactive Orbitrap (Thermo Scientific) mass spectrometer coupled to an Ultimate 3000 RSLC system (Dionex). The liquid chromatography system was fitted with either a ZIC-HILIC column (150 mm × 4.6 mm) or a ZIC-pHILIC column (150 mm × 2.1 mm) and respective guard columns (20 mm × 2.1 mm) (all Merck, Germany)[23]. For the ZIC-HILIC column the flow rate was 300 µl min^{-1} and the gradient comprised 0.1% formic acid/water and 0.1% formic acid/acetonitrile as follows (time (min), % acetonitrile): 0, 80; 12, 50; 26, 50; 28, 20; 36, 20; 37, 80; 45, 80. For the ZIC-pHILIC column the flow rate was 200 µl min^{-1} and the gradient comprised 20 mM $(NH_4)_2CO_3$, pH 9.4 and acetonitrile as follows (time (min), % acetonitrile): 0, 80; 2, 80; 17, 20; 17.1, 80; 19.1, 80; 22.1, 80;22.2, 80, with an increase in flow rate to 400 µl min^{-1} from 19.1 to 22.1. The mass spectrometer was operated in full MS and polarity switching mode. Samples were randomized in order to avoid bias due to machine drift and processed blindly. The acquired spectra were analysed using XCalibur Qual and XCalibur Quan Browser software (Thermo Fisher Scientific) by referencing to an internal library of compounds. Absolute quantification of selected metabolites was performed by interpolation of the corresponding standard curve obtained from serial dilutions of commercially available standards (Sigma Aldrich) running with the same batch of samples. All the extractions and analyses were done under the same conditions and relative to the same internal standard. The NADH/NAD^+, lactate/pyruvate and succinate/fumarate ratios are presented as relative changes in the ratio of the ion current for these metabolites, which is proportional to, but not the same as, the true ratio of the metabolite levels.

LC–MS/MS analysis of succinate and malonate from pig, mouse and human temperature studies and fumarate delivery from *bis*-acetoxymethyl fumarate in cells was performed using an LCMS-8060 mass spectrometer (Shimadzu, UK) with a Nexera X2 UHPLC system (Shimadzu, UK). Samples were stored in a refrigerated autosampler (4 °C) upon injection of 5 µl into a 15-µl flow-through needle. Separation was achieved using a SeQuant ZIC-HILIC column (3.5 µm, 100 Å, 150 × 2.1 mm, 30 °C column temperature; MerckMillipore, UK) with a ZIC-HILIC guard column (200 Å, 1 × 5 mm). A flow rate of 200 µl min^{-1} was used with mobile phases of A) 100 mM ammonium acetate (pH 6.9) and B) 100% acetonitrile. A gradient of 0–0.1 min, 80% MS buffer B; 0.1–4 min, 80%-20% B; 4–10 min, 20% B, 10–11 min, 20–80% B; 11–15 min, 80% B was used. The mass spectrometer was operated in negative ion mode with multiple reaction monitoring (MRM) and spectra were acquired using Labsolutions software (Shimadzu, UK), with compound quantities calculated from relevant standard curves (succinate, malonate or fumarate) in MS extraction buffer and comparing against [^{13}C] succinate (for succinate and fumarate) or [^{13}C]malonate (for malonate) internal standards. Metabolomic data have been uploaded as study MTBLS1085 to MetaboLights (https://www.ebi.ac.uk/metabolights).

Tissue analysis for ATP/ADP ratio. ATP and ADP concentrations were measured using a luciferase-based assay[24]. Frozen tissue samples were homogenized in ice-cold perchloric acid extractant (3% vol/vol $HClO_4$, 2 mM Na_2EDTA, 0.5% Triton X-100). The supernatant was diluted to a concentration of 1 mg frozen tissue per ml. Samples, ATP and ADP standards were pH neutralized using a potassium hydroxide solution (2 M KOH, 2 mM Na_2EDTA, 50 mM MOPS), vortexed until formation of a white precipitate ($KClO_4$), then centrifuged (17, 000 × g for 1 min at 4 °C). For ADP measurements, 250 µl neutralized sample supernatant was mixed with 250 µl ATP sulfurylase assay buffer (20 mM Na_2MoO_4, 5 mM GMP, 0.2 U ATP sulfurylase (New England Biolabs), in Tris-HCl buffer (100 mM Tris-HCl, 10 mM $MgCl_2$ (pH 8.0))), incubated for 30 min at 30 °C with shaking (500 r.p.m.), heated at 100 °C for 5 min and then cooled on ice. Standards (100 µl), samples for ATP measurement (100 µl) or samples for ADP measurement (200 µl) (in duplicate) were added to 400 µl Tris-acetate (TA) buffer (100 mM Tris, 2 mM Na_2EDTA, 50 mM $MgCl_2$, pH 7.75 with glacial acetic acid) in luminometer tubes. 10 µl pyruvate kinase solution (100 mM PEP, 6 U pyruvate kinase suspension (Sigma # P1506)) was added to one set of samples for ADP measurement and incubated for 30 min at 25 °C in the dark to convert ADP to ATP. The other duplicate tube (without addition of pyruvate kinase solution) served as an ADP 'blank' value. The samples were then all assayed for ATP content in a Berthold AutoLumat Plus luminometer by addition of 100 µl Luciferase/Luciferin Solution (7.5 mM DTT, 0.4 mg ml^{-1} BSA, 1.92 µg luciferase ml^{-1} (SIGMA no, L9506), 120 µM D-luciferin (SIGMA no. L9504), made in TA buffer (25% vol/vol glycerol)), delivered via auto injection, protected from light. Bioluminescence of the ATP-dependent luciferase activity was measured for 45 s post injection and the data quantified against standard curves.

Glycogen assay. The glycogen assay protocol was adapted from ref. [25], and measured the production of NA(D)PH during the oxidation of glycogen-derived glucose to 6-phosphogluconate. Frozen tissue (5–10 mg) was minced finely before being treated with 250 µl hot acid (2 M HCl; 100 °C) or alkali (2 M NaOH; 100 °C) to hydrolyse glycogen or as an unhydrolysed control respectively (100 °C, 1 h, vigorous shaking every 10 min). Samples were subsequently cooled to RT and neutralized to pH 7 with either 2 M NaOH or HCl and the addition of 500 µl 400 mM Tris (pH 7.4). Neutralized samples were vortexed before centrifuging (17,000 × g, 10 min, RT). 60 µl of sample supernatant was plated in duplicate in a 96-well plate together with a glucose standard curve (0,10, 20, 40, 80, 160 µg glucose ml^{-1}). 200 µl glucose assay reagent (G3293, Sigma) was added to each well and the plate incubated (5 min, RT) prior to measuring absorbance at 340 nm in a Spectramax Plus 384 plate reader (Molecular Devices, UK). The average absorbance of each sample was interpolated using the standard curve and multiplied by the final volume after pH adjustment to give µg of glycogen (or glucose for NaOH control) in original sample. This was divided by the weight of tissue added and the NaOH control was subtracted from the HCl sample to give µg glycogen per mg frozen tissue.

Synthesis of bis(acetoxymethyl)succinate. Bis(acetoxymethyl)succinate (202 mg, 0.769 mmol) was prepared in 91% yield from succinic acid (100 mg, 0.847 mmol) in a similar way to Ehinger et al.[17] except acetonitrile was used as solvent, and after 16-h reaction the solvent was evaporated and the crude mixture purified by column chromatography (SiO_2, hexane-ethyl acetate (7:3)). R_f (SiO_2, hexane-ethyl acetate (7:3)) = 0.24. ν_{max} (ATR): 1751 (CO) cm^{-1}. δ_H (400 MHz, $CDCl_3$): 5.75 (4H, s, OCH_2O), 2.71 (4H, s, CH_2CO_2), 2.12 (6H, s, CH_3). δ_C (126 MHz, $CDCl_3$): 170.93 (2C, s, CO), 169.71 (2C, s, CO), 79.38 (2C, s, CH_2O), 28.66 (2C, s, CH_2CO), 20.80 (2C, s, CH_3). LRMS (ESI^+): 285 (MNa^+, 100%). HRMS (ESI^+): 285.0579. $C_{10}H_{14}NaO_8^+$ requires (MNa^+), 285.0581. ^1H nuclear magnetic resonance (NMR) and ^{13}C NMR data agree with the literature[17]. See Supplementary Fig. 1. The original data have been deposited at https://doi.org/10.5525/gla.researchdata.646.

Synthesis of bis(acetoxymethyl) fumarate. Bromomethyl acetate (300 µl, 3.06 mmol, 2.2 equivalents) was added to a solution of fumaric acid (161 mg, 1.39 mmol, 1.0 eq) and diisopropylamine (605 µl, 3.47 mmol, 2.5 eq) in dry acetonitrile (8 ml) cooled to 0 °C under argon. The solution was allowed to warm to room temperature, stirred overnight, concentrated under vacuum and purified by column chromatography (SiO_2, hexane-ethyl acetate (80:20) to (50:50)) to give the bis-AM ester as a white solid (310 mg, 86%). R_f (SiO_2, hexane-ethyl acetate (7:3)) = 0.31. M.p. 89–91 °C. ν_{max} (ATR) cm^{-1}: 1755 (CO_2), 1728 (CO_2), 977 (C=C). δ_H (400 MHz: $CDCl_3$): 2.12 (6H, s, CH_3), 5.84 (CH_2), 6.92 (CH). δ_C (100 MHz: $CDCl_3$): 20.76 (CH_3), 79.80 (CH_2), 133.98 (CH), 163.27 (C), 169.51 (C). HRMS (ESI^+): 283.0423. $C_{10}H_{12}NaO_8$ requires (MNa^+), 283.0424. See Supplementary Fig. 1. The original data have been deposited at https://doi.org/10.5525/gla.researchdata.646.

Troponin measurement. Non-heparinized IVC blood samples were taken immediately prior to graft collection. Samples were left for 30 min at room temperature to ensure adequate clot propagation, centrifuged (2,000 × g for 10 min) and serum apportioned into aliquots and stored at −80 °C. Serum troponin-I was measured using a commercially available mouse cardiac troponin-I ELISA (KT-470, Kamiya Biomedical Company, Seattle, WA, USA) by the Core Biomedical Analysis Laboratory, Addenbrooke's Hospital, Cambridge.

Measurement of mtDNA release. The release of mitochondrial and nuclear DNA into the circulation was assessed using the droplet digital polymerase chain reaction (ddPCR). Serum samples were centrifuged (1,600*g* for 10 min) and the supernatant was then centrifuged once more (16,000*g* for 10 min), and DNA was isolated using the DNeasy Blood kit (QIAGEN) according to the manufacturer's instructions, with step 3, the addition of lysis buffer AL, omitted. DNA was quantified using a 'Nanodrop' system and diluted to 1 ng μL^{-1} in elution buffer. For mtDNA, the *Nd5* gene was assessed using the following primers: F- CTGCTCTTTCCCAGACGAGG; R-AAGGCCACTTATCACCAGC. For nuclear DNA, the *Actb* gene was assessed, using F-ACCTAATTAAACACATCAACTTCCC; R- GACTCAGTGCCAGGTTGTAA. Each PCR reaction (22 µl) comprised 1 µl (= 1 ng) DNA template, 11 µl ddPCR Supermix (no dUTP) containing Taq, 314 nM of each primer, and 210 nM of the HEX-ND5 probe (ACACCACCACATCAATCAAATTCTCCTTCA) and of the FAM-β-actin probe (ATTGCCTTTCTGACTAGGTG) and then made up to 22 µl with H_2O. The BIORAD ddPCR AutoDG was used to generate ddPCR droplets, and the plate was sealed at 174 °C before the PCR was run in a BIORAD C1000 Thermo Cycler: 95 °C at 10 min followed by 40 cycles of 30 sec at 95 °C and 1 min at 58 °C and then 95 °C at 10 min. After completion of the PCR, the fluorescence of the FAM and HEX probes was measured using the BIORAD QX200 Droplet Reader and analysed using the BIORAD Quantilife software and Excel.

qPCR assay for mtDNA damage. qPCR to detect murine mtDNA lesions was based on ref. [26] and performed using the following primers at 10 µM: forward primer FWD: 5′-GCCAGCCTGACCCATAGCCATAAT-3′. The reverse primer for the long 10090-bp PCR product was: REV: 5′-GAGAGATTTTATGGGTGTAATGCGG-3′. The reverse primer for the short 127-bp PCR product was: REV: 5′-GCCGGCTGCGTATTCTACGTTA-3′. Sample DNA was extracted using the QIAmp blood and tissue kit following the provided instructions. qPCR was performed on 15 ng DNA in 35-µl reactions on a PCR thermocycler (Biometra). 1 U TaKaRa LA Taq was used per reaction. PCR master mix was prepared following the TaKaRa LA Taq instructions. Linearity of the PCR reaction was confirmed for each sample by running a 1:2 diluted sample simultaneously. Cycling parameters for the short reaction were 94 °C for 5 min, followed by 16 cycles of 94 °C for 30 s, 64 °C for 45 s, 72 °C for 45 s, followed by 72 °C for 10 minutes. Conditions for the long amplification were 94 °C for 5 minutes followed by 18 cycles of 94 °C for 15 s and 64 °C for 12 min, followed by 72 °C for 10 min. The PCR reaction was confirmed on 1% agarose gels and concentrations of the PCR product were determined by measuring the emission of the samples at 488 nm and excitation at 525 nm after picogreen addition at 1:200 dilution.

Cell culture. C2C12 mouse myoblast cells were plated at 300,000 cells per well in 6-well plates and left to adhere overnight. The following day, cells were treated with 0 (DMSO vehicle control), 0.25, 0.5 or 1 mM fumarate-AM diester for 30 min at 37 °C. Cells were washed 4 times with ice-cold PBS prior to extraction with 500 µl extraction buffer containing [^{13}C]succinate internal standard for 15 min on dry ice. Cells were scraped and transferred to microcentrifuge tubes prior to agitation (15 min, 4 °C, 1,000 r.p.m.), and incubation (−20 °C, 1 h). Samples were centrifuged (17,000*g*, 10 min, 4 °C), the supernatant transferred to fresh microcentrifuge tubes and recentrifuged (17,000*g*, 10 min, 4 °C). The resulting supernatant was transferred to glass MS vials and stored at −80 °C until analysis by LC–MS/MS. Fumarate levels were determined by interpolation of a fumarate standard curve and normalized to cellular protein by BCA assay of a parallel treated plate.

Statistics and experimental design. All data in figures are presented as mean values ± s.e.m. unless otherwise stated. Statistical analysis was performed between two groups using Student's *t*-test with sometimes using Sidak's post-test for multiple comparisons, and between multiple groups by one-way analysis of variance (ANOVA) or two-way ANOVA with Bonferroni's or Tukey's multiple comparison testing. A *P* value of less than 0.05 was considered significant. For Fig. 2, fold changes in metabolite abundances (and their statistical significance) between time points were calculated by using linear modelling with an empirical Bayes approach as implemented in the 'limma' package of R (ref. [27]). Regularized logs were taken of the abundance measurements of each metabolite, then the targets and the design matrix were defined for groups of samples to be compared, and the data fitted to a linear model. Contrasts were defined and significantly affected metabolites were identified from the fitted model by using their *P* values, adjusting for multiple-testing by using the Benjamini–Hochberg procedure. Volcano plots were produced by plotting the fold-change of each metabolite versus its adjusted *P* value in R.

Reporting summary. Further information on research design is available in the Nature Research Reporting Summary linked to this article.

Data availability

Metabolomic data have been uploaded as study MTBLS1085 to MetaboLights (https://www.ebi.ac.uk/metabolights). The original synthetic chemistry data have been deposited at https://doi.org/10.5525/gla.researchdata.646. Other data that support the findings of this study are available from the corresponding author upon reasonable request.

Received: 4 March 2019; Accepted: 16 August 2019;
Published online: 30 September 2019

References

1. Jahania, M. S., Sanchez, J. A., Narayan, P., Lasley, R. D. & Mentzer, R. M. Jr. Heart preservation for transplantation: principles and strategies. *Ann. Thorac. Surg.* **68**, 1983–1987 (1999).
2. Southard, J. H. & Belzer, F. O. Organ preservation. *Annu. Rev. Med.* **46**, 235–247 (1995).
3. Chouchani, E. T. et al. A unifying mechanism for mitochondrial superoxide production during ischemia-reperfusion injury. *Cell Metab.* **23**, 254–263 (2016).
4. Chouchani, E. T. et al. Ischaemic accumulation of succinate controls reperfusion injury through mitochondrial ROS. *Nature* **515**, 431–435 (2014).
5. Pagani, F. D. Use of heart donors following circulatory death: a viable addition to the heart donor pool. *J. Am. Coll. Cardiol.* **73**, 1460–1462 (2019).
6. Johnson, R. J., Bradbury, L. L., Martin, K. & Neuberger, J. Organ donation and transplantation in the UK-the last decade: a report from the UK national transplant registry. *Transplantation* **97**, S1–S27 (2014).
7. Chew, H. C. et al. Outcomes of donation after circulatory death heart transplantation in australia. *J. Am. Coll. Cardiol.* **73**, 1447–1459 (2019).
8. Dhital, K. K. et al. Adult heart transplantation with distant procurement and ex-vivo preservation of donor hearts after circulatory death: a case series. *Lancet* **385**, 2585–2591 (2015).
9. Nasralla, D. et al. A randomized trial of normothermic preservation in liver transplantation. *Nature* **557**, 50–56 (2018).
10. Coffey, J. C. et al. The influence of functional warm ischemia time on DCD liver transplant recipients' outcomes. *Clin. Transplant.* **31**, e13068 (2017).
11. Blok, J. J. et al. Longterm results of liver transplantation from donation after circulatory death. *Liver Transplant.* **22**, 1107–1114 (2016).
12. Eltzschig, H. K. & Eckle, T. Ischemia and reperfusion—from mechanism to translation. *Nat. Med.* **17**, 1391–1401 (2011).
13. Liu, F. & Kang, S. M. Heterotopic heart transplantation in mice. *J. Vis. Exp.* **6**, 238 (2007).
14. Niimi, M. The technique for heterotopic cardiac transplantation in mice: experience of 3000 operations by one surgeon. *J. Heart Lung Transplant.* **20**, 1123–1128 (2001).
15. Zhang, Q. et al. Circulating mitochondrial DAMPs cause inflammatory responses to injury. *Nature* **464**, 104–107 (2010).
16. Nakahira, K. et al. Circulating mitochondrial DNA in patients in the ICU as a marker of mortality: derivation and validation. *PLoS Med.* **10**, e1001577 (2013).
17. Ehinger, J. K. et al. Cell-permeable succinate prodrugs bypass mitochondrial complex I deficiency. *Nat. Commun.* **7**, 12317 (2016).
18. Valls-Lacalle, L. et al. Selective inhibition of succinate dehydrogenase in reperfused myocardium with intracoronary malonate reduces infarct size. *Sci. Rep.* **8**, 2442 (2018).
19. Valls-Lacalle, L. et al. Succinate dehydrogenase inhibition with malonate during reperfusion reduces infarct size by preventing mitochondrial permeability transition. *Cardiovasc. Res.* **109**, 374–384 (2016).
20. Bundgaard, A. et al. Metabolic adaptations during extreme anoxia in the turtle heart and their implications for ischemia-reperfusion injury. *Sci. Rep.* **9**, 2850 (2019).
21. Zhang, J. et al. Accumulation of succinate in cardiac ischemia primarily occurs via canonical krebs cycle activity. *Cell Rep.* **23**, 2617–2628 (2018).
22. Dare, A. J. et al. The mitochondria-targeted anti-oxidant MitoQ decreases ischemia-reperfusion injury in a murine syngeneic heart transplant model. *J. Heart Lung Transplant.* **34**, 1471–1480 (2015).
23. Mackay, G. M., Zheng, L., van den Broek, N. J. & Gottlieb, E. Analysis of cell metabolism using LC-MS and isotope tracers. *Meth. Enzymol.* **561**, 171–196 (2015).
24. Strehler, B. L. in *Methods in Enzymatic Analysis* (ed. Bergmeyer, U.) 2112–2126 (Academic Press, 1974).
25. Passonneau, J. V. & Lauderdale, V. R. A comparison of three methods of glycogen measurement in tissues. *Anal. Biochem.* **60**, 405–412 (1974).
26. Santos, J. H., Meyer, J. N., Mandavilli, B. S. & Van Houten, B. Quantitative PCR-based measurement of nuclear and mitochondrial DNA damage and repair in mammalian cells. *Methods Mol. Biol.* **314**, 183–199 (2006).
27. Ritchie, M. E. et al. Limma powers differential expression analyses for RNA-sequencing and microarray studies. *Nuc. Acids Res.* **43**, e47 (2015).

Acknowledgements

Work in the M.P.M. laboratory was supported by the Medical Research Council UK (MC_U105663142) and by a Wellcome Trust Investigator award (110159/Z/15/Z) to M.P.M. Work in the C.F. laboratory was supported by the Medical Research Council (MRC_MC_UU_12022/6). Work in the K.S.P. laboratory was supported by the Medical Research Council UK. Work in the RCH lab laboratory was supported by a Wellcome Trust Investigator award (110158/Z/15/Z) and a PhD studentship for .L.P from the University of Glasgow. A.V.G. was supported by a PhD studentship funded by the National Institute for Health Research Blood and Transplant Research Unit (NIHR BTRU) in Organ Donation and Transplantation at the University of Cambridge in collaboration with Newcastle University and in partnership with NHS Blood and Transplant (NHSBT). The views expressed are those of the author(s) and not necessarily those of the NHS, the NIHR, the Department of Health or NHSBT. We are grateful to the donors, the donor families, National Health Service Blood transfusion and Transplantation, and the Cambridge Biorepository for Translational Medicine for access to human samples.

Author contributions

J.L.M., A.S.H.C., K.S.-P., R.C.H., T.K., M.H., K.M., C.F. and M.P.M. designed the experimental protocols. A.V.G., F.M.A., H.A.P., S.T.C., L.T., M.M.H., E.C.H., A.S.H.C., T.E.B., L.P., A.L., E.N. and J.L.M. performed the studies. J.L.M., A.S.H.C., A.M.J. and A.R. analysed the data. J.L.M., A.S.H.C., K.S.-P., C.F. and M.P.M. wrote the manuscript with assistance from all the other authors.

Competing interests

M.P.M., T.K. and R.C.H. have submitted a patent application on the use of dimethyl malonate to prevent IR injury.

Additional information

Extended data is available for this paper at https://doi.org/10.1038/s42255-019-0115-y.

Supplementary information is available for this paper at https://doi.org/10.1038/s42255-019-0115-y.

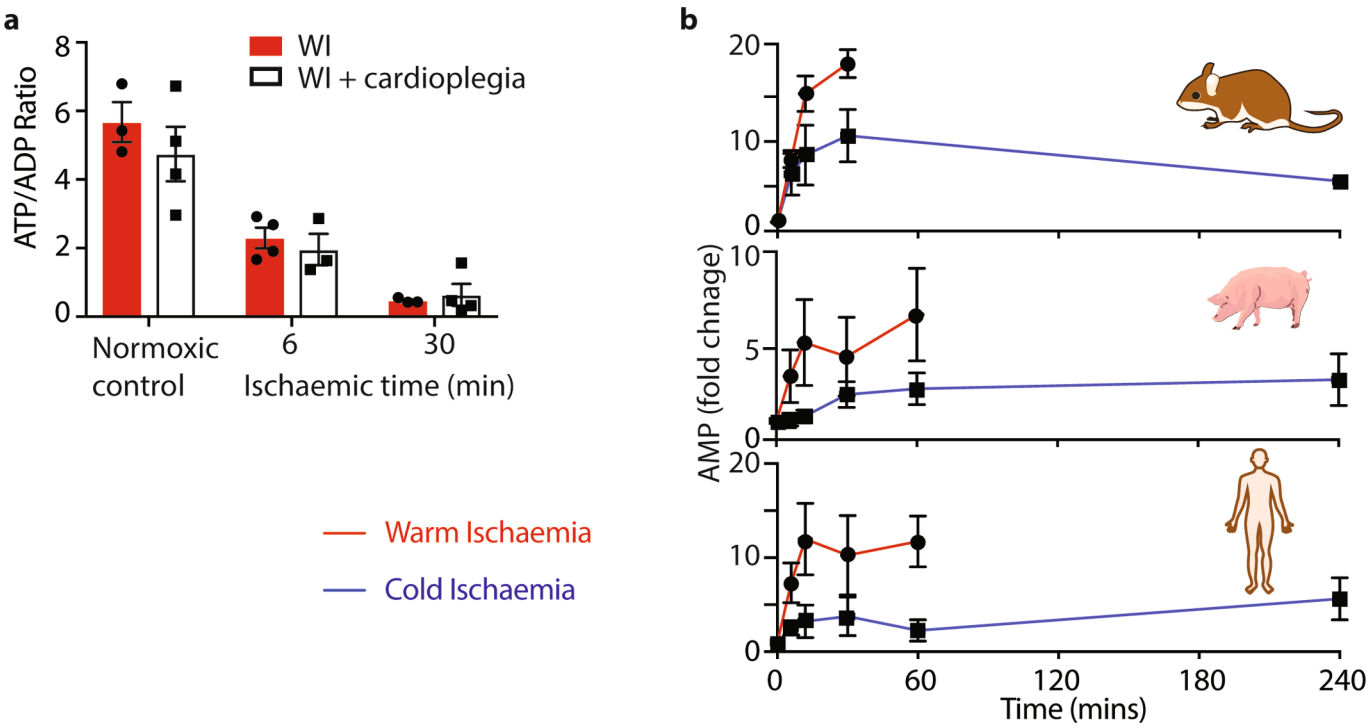
Correspondence and requests for materials should be addressed to M.P.M.

Peer review information Primary Handling Editor: Ana Mateus.

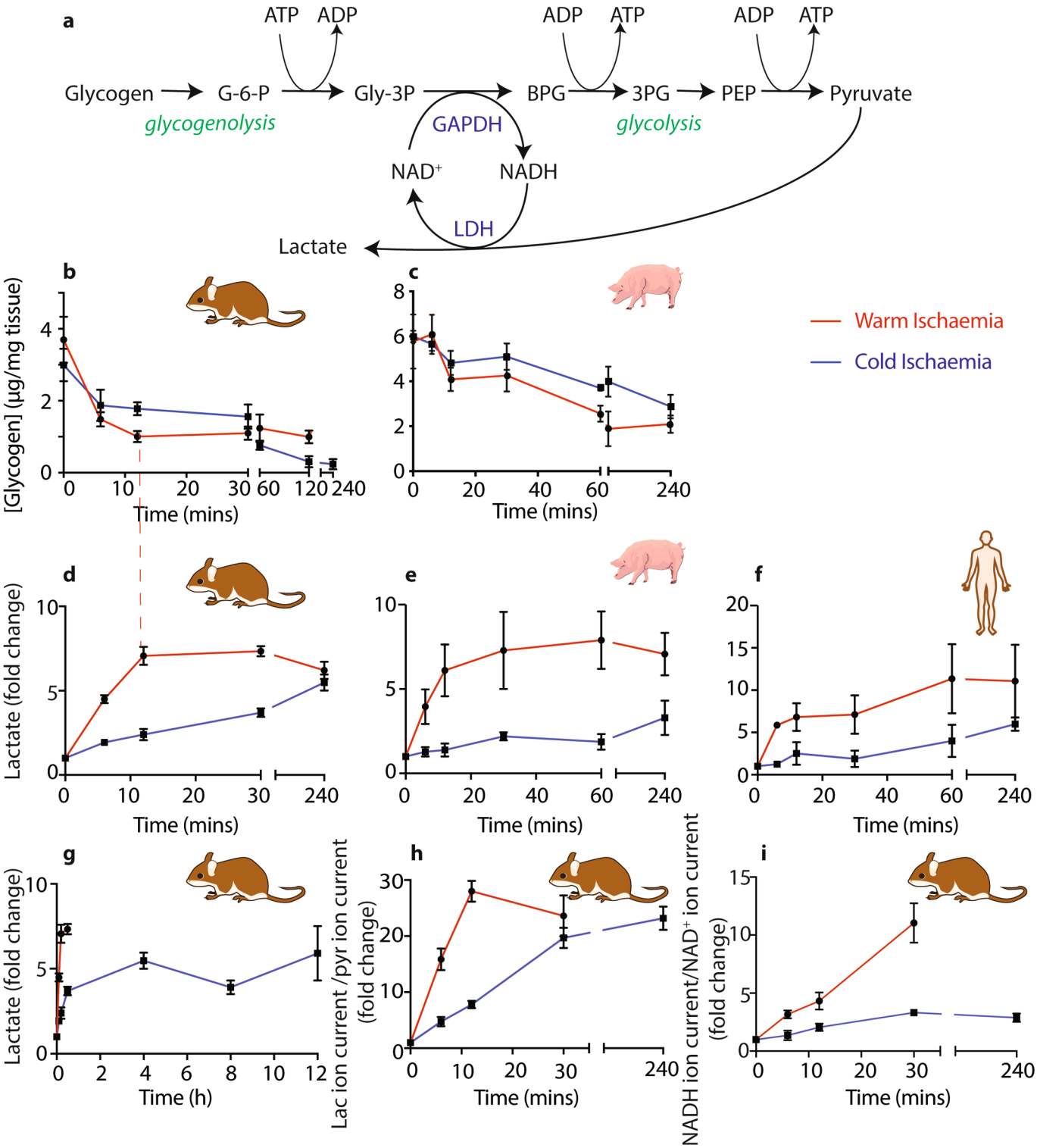
Reprints and permissions information is available at www.nature.com/reprints.

Publisher's note Springer Nature remains neutral with regard to jurisdictional claims in published maps and institutional affiliations.

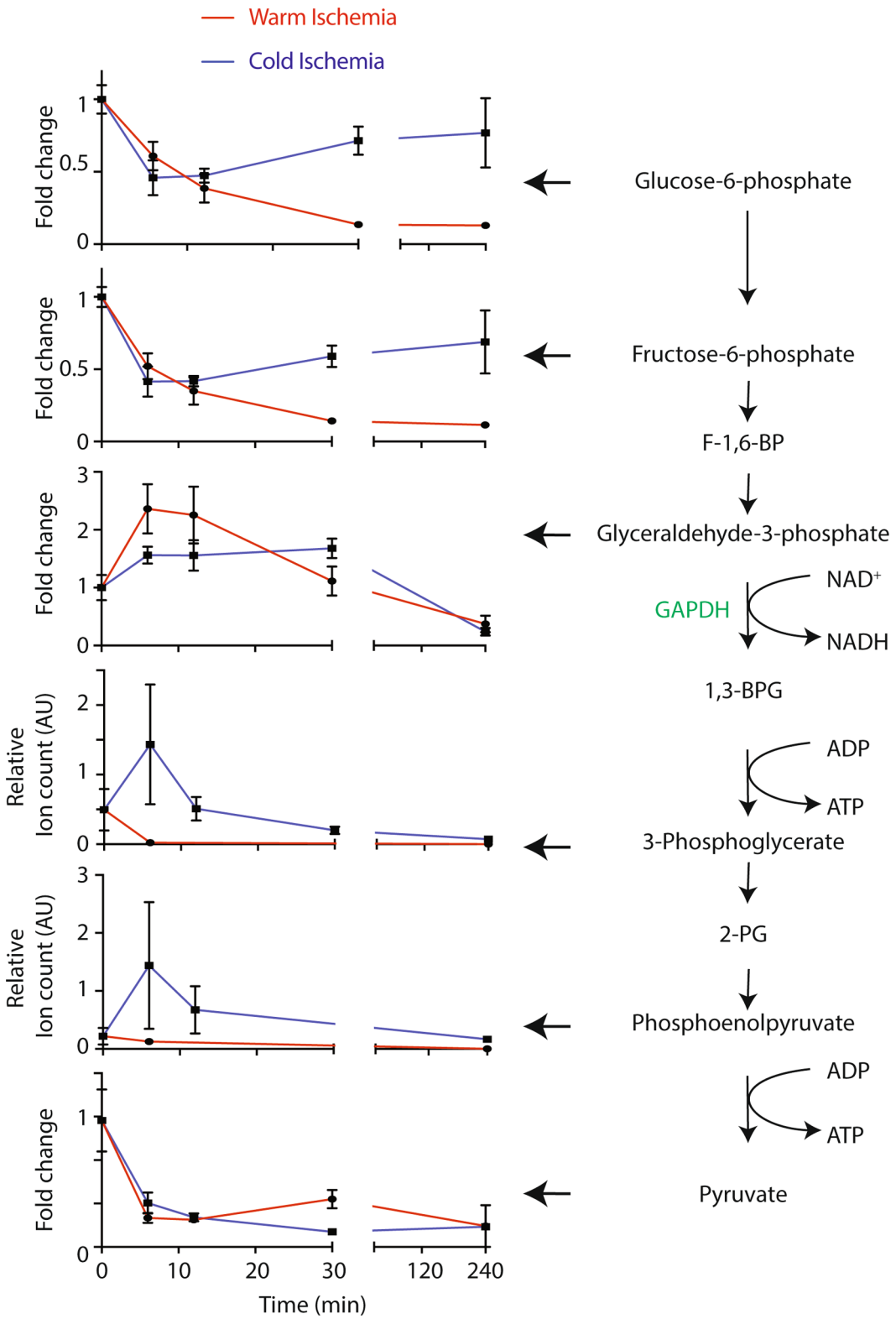
© The Author(s), under exclusive licence to Springer Nature Limited 2019



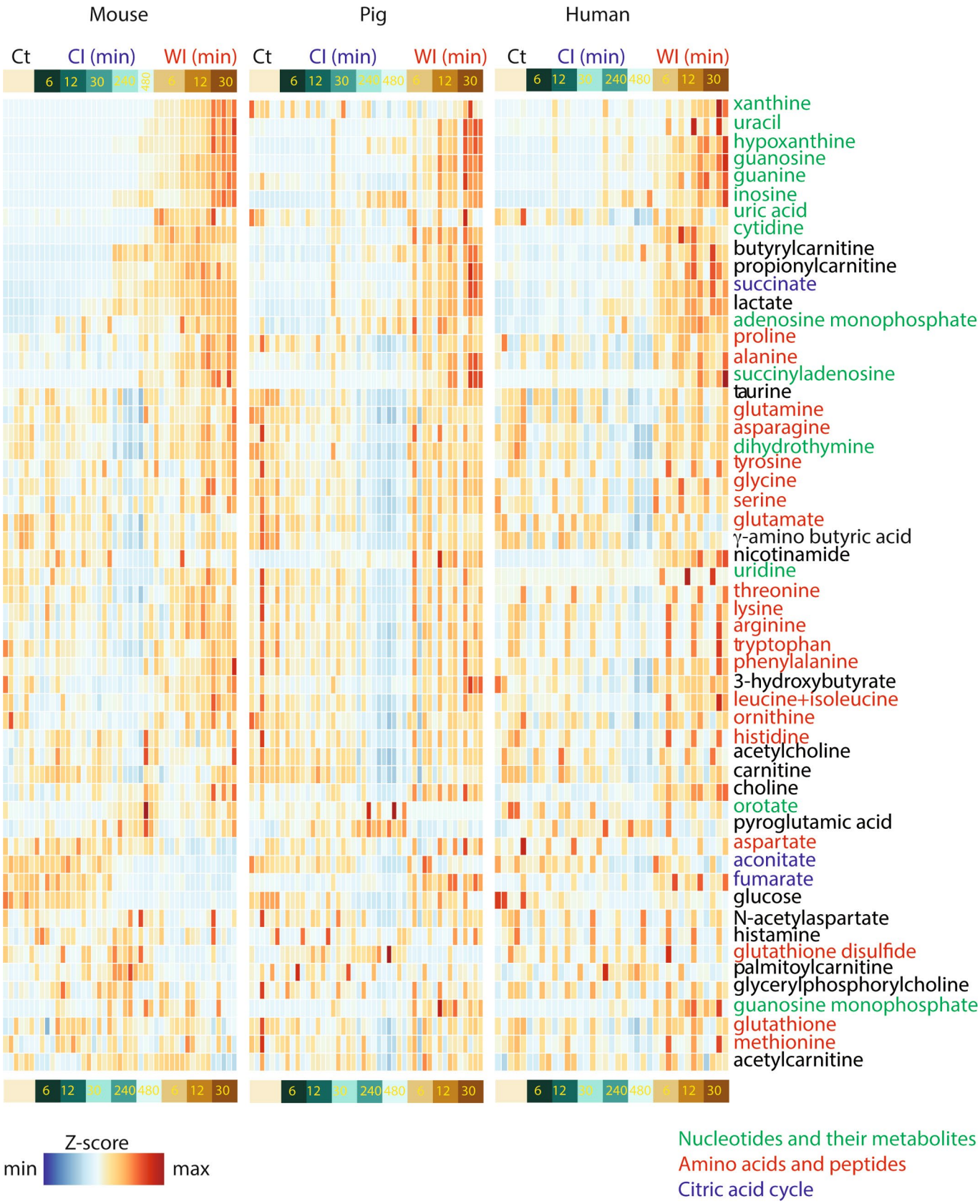
Extended Data Fig. 1 | Effect of cardioplegia on ATP/ADP during WI in the mouse heart and cardiac AMP fold change during WI and CI. a, ATP/ADP ratios of mouse hearts were assessed as described in Fig. 1 during WI ± cardioplegia at the onset of WI. Individual normoxic controls were used for WI ± cardioplegia, 6 min, n = 3; all others n = 4. Data are means ± SEM, WI, normoxic control and 12 min, and WI + cardioplegia, *n* = 3–4. **b**, AMP levels were determined in heart tissue after various times of WI or CI and are given as fold change relative to normoxic controls. Data are means ± s.e.m. Mouse normoxic controls, *n* = 11; CI, 240 min; *n* = 4; all others *n* = 5. *n* = 5 (pig), 4 (human).



Extended Data Fig. 2 | Glycogen and glycolysis during WI and CI. a, Glycogenolysis and glycolysis in ischaemia. G-6-P, glucose-6-phosphate; Gly-3P, glyceraldehyde-3 phosphate; BPG, bisphosphoglycerate; 3PG, 3-phosphoglycerate; GAPDH, glyceraldehyde-3-phosphate dehydrogenase; LDH, lactate dehydrogenase; PEP, phosphoenolpyruvate. **b**,**c**, Heart glycogen during WI and CI in (**b**) mouse and (**c**) pig. Mean ± s.e.m. Pig, $n=3$. Mouse, WI, 0, 6, 12, 30 min, $n=5$; 120 min, $n=4$; CI, 6, 12, 30, 60 min, $n=7$; 120 and 240 min, $n=3$. **d**–**g**, Heart lactate levels during WI and CI in (**d**,**g**) mouse, (**e**) pig and (**f**) human. Dashed red line shows when both glycogenolysis and lactate accumulation stop during WI. Data are shown as the fold-change relative to normoxic controls, mean ± SEM, $n=4$. **h**, Heart lactate/pyruvate ion current ratio during WI and CI in the mouse, determined as fold change relative to normoxic controls. Data are relative changes in the ratio of the ion current for these metabolites. Mean ± s.e.m. Normoxic controls $n=11$, WI, $n=5$; CI, $n=4$. **i**, Heart NADH/NAD^{++} ion current ratio during WI and CI in the mouse, shown as fold change relative to normoxic controls. Data are presented as relative changes in the ratio of the ion current for these metabolites, which is proportional to, but not the same as, the true ratio of the metabolite levels. Data mean ± s.e.m. Normoxic controls $n=11$, WI, $n=5$; CI, $n=4$. NADH was not detectable in two control hearts and the lowest detectable value was then used.



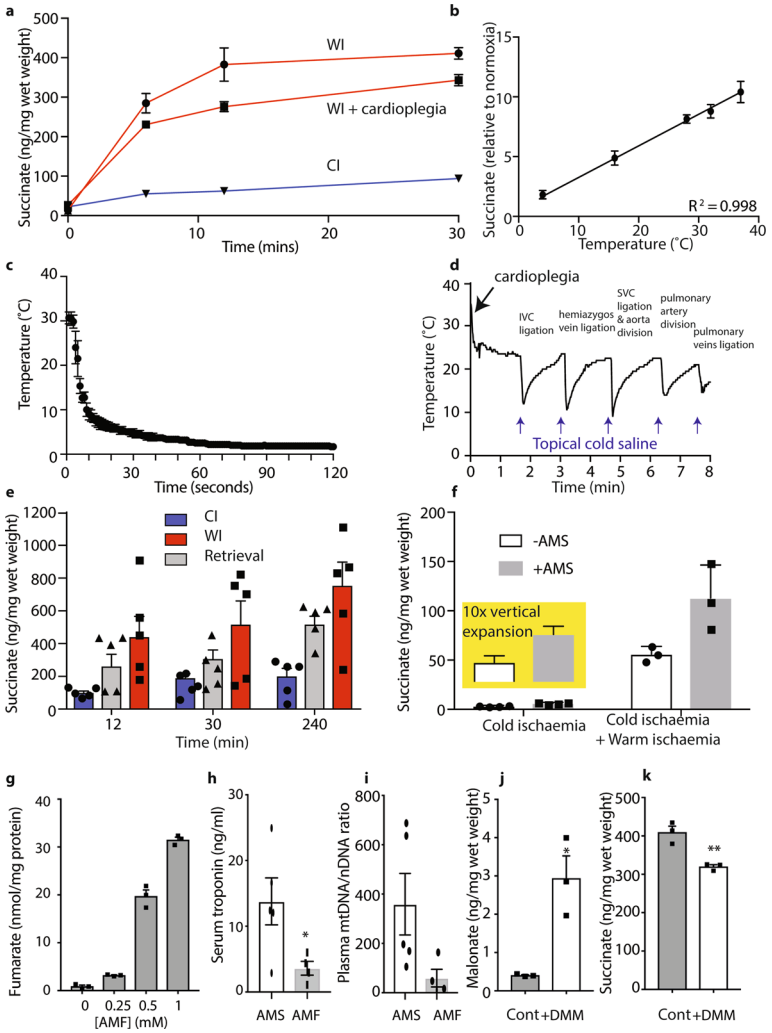
Extended Data Fig. 3 | Changes in glycolytic metabolites in the mouse heart during WI and CI. Plots of the glycolytic metabolites detected in the mouse heart during WI and CI. Heart tissue was stored and analysed as described in Fig. 4. In most cases data are shown relative to normoxic control tissues. In some cases where the metabolite was undetectable in normoxic tissue the ion currents in arbitrary units (AU) are reported. Data are means ± s.e.m. For glucose -6-phosphate and fructose-6-phosphate, normoxic control, $n=11$; 240 min, $n=4$; rest, $n=5$. For glyceraldehyde-3-phosphate, normoxic control, $n=11$; 240 min WI, $n=4$; 30 and 240 min CI, $n=3$; rest, $n=5$. Pyruvate was poorly detected, normoxic control, $n=11$; WI, 6 min I, $n=4$; 12 min, $n=1$; 30 min, $n=2$; 240 min, n = 4; CI, WI, 6 min, n = 5; 12 min, $n=4$; 30 min, $n=2$, 240 $n=1$. For 3-phosphoglycerate and phosphoenol pyruvate ion counts were used, and for the normoxic control, $n=8$. The ion counts for WI samples were either undetectable (no data point symbol) or $n=1$ (data point sysmbol). For CI $n=3$ for both compounds at 6 and 12 min, and $n=1$ for 240 min. Phosphoenol pyruvate was not detected at 30 min and for 3-phosphoglycerate $n=1$ at 30 min. F-1,6-BP, fructose 1,6-bisphosphate; 2-PG, 2-phosphoglycerate; GAPDH, glyceraldehyde-3-phosphate dehydrogenase; AU, arbitrary units.



Extended Data Fig. 4 | Metabolic changes during WI and CI. Heat maps showing how 54 metabolites change in relative abundance during WI and CI in mouse, pig and human heart tissue compared to normoxic controls (Ct). Independent biological replicates for each condition are: mouse, Ct and WI 6 min, $n=6$; CI, 480 min, $n=3$; rest, $n=5$. Pig, $n=5$. Human, Ct, $n=5$; rest, $n=4$.



Extended Data Fig. 5 | Extended set of metabolic changes during WI and CI in mice. Heat map showing how 107 metabolites change in relative abundance in mouse hearts during WI and CI compared to normoxic controls (Ct). Independent biological replicates for each condition are: Ct, $n=6$ and WI 6 min; 480 min CI, $n=3$; rest, $n=5$.



Extended Data Fig. 6 | Time course of cardioplegia, flushing, temperature and succinate changes in the heart. Succinate levels in mouse hearts were assessed as described in Fig. 3 during CI and WI ± cardioplegia at the onset of WI. Individual normoxic controls were used for CI and for WI ± cardioplegia. Data are means ± s.e.m. WI + cardioplegia, $n = 3$, rest $n = 4$. **b**, Mouse hearts were exposed and diastolic arrest was induced with St Thomas' cardioplegia solution. Hearts were then rapidly excised and placed in storage medium at various temperatures, and after 12 min were rapidly . The succinate level was determined and is expressed relative to the amount in normoxic control hearts (data = means ± s.e.m., $n = 4$). There was a linear relationship between temperature and succinate accumulation ($R^2 = 0.998$). **c**, Mouse hearts were rapidly excised as in **b** and placed in storage medium at 4 °C. The temperature of the apexes of the hearts were measured during cooling using a thermocouple placed into the apex of the heart through the ascending aorta. Mean ± s.e.m. ($n = 3$). **d**, Mouse hearts were retrieved by surgical preparation of the great vessels required for heterotopic heart transplantation and the temperature of the apex measured using a thermocouple. Diastolic arrest of mouse hearts was induced with cold St Thomas' cardioplegia solution and topical cold saline was applied at the start of the retrieval process and then at regular intervals thereafter (blue arrows). The panel shows a typical result of three replicates. **e**, Succinate measured in hearts under WI, CI or standard retrieval (as described in **d**). Data are mean ± s.e.m., $n = 5$. **f**, Diacetoxymethyl succinate (AMS) administration and tissue succinate content. Mice were anaesthetized under isoflurane anaesthesia and a laparotomy was performed to expose the great vessels. The inferior vena cava (IVC) was infused with a bolus of 500 µl St Thomas' cardioplegia solution and 5% DMSO ± 3.2 mg AMS. Immediately after administering the cardioplegia, the thorax of the mouse was opened and the heart rapidly removed and placed in ice cold PBS (this step took between 10–20 s). The hearts were stored in ice cold PBS for 30 min and then either clamp frozen in liquid nitrogen or were then incubated for a further 20 min at 37 °C in the carcass of the animal to mimic organ anastomosis and then were clamp frozen in liquid nitrogen. Absolute tissue succinate concentration was quantified by interpolation of the standard curve obtained from serial dilutions of commercially available standards that were run with the same batch of samples. Data mean of 4 hearts per conditions ± s.e.m. **g**, Effect of diacetoxymethyl fumarate (AMF) administration on cell levels of fumarate. C2C12 cells were incubated with 0, 0.25, 0.5 or 1 mM fumarate-AM diester for 30 min at 37 °C before extraction and analysis of fumarate by LC–MS/MS (mean ± s.e.m., $n = 3$ biological replicates). **h**,**i**, Comparison of AMF administration with that of AMS. Mice were anaesthetized under isoflurane anaesthesia and a laparotomy was performed to expose the great vessels. The inferior vena cava (IVC) was infused with a bolus of 500 µl St Thomas' cardioplegia solution and 5% DMSO + 3.2 mg AMS or 30% DMSO + 3.18 mg AMF, which is equimolar with the dose of AMS used. Immediately after administering the cardioplegia, the thorax of the mouse was opened and the heart was rapidly removed and placed in ice-cold PBS (this step took between 10–20s). The hearts were stored in ice cold PBS for 30 min and then transplanted into a recipient as described in the legend to Fig. 4d. After 24 h, the plasma levels of troponin (**h**) and mtDNA relative to nuclear DNA (**i**) were assessed. Data are the mean of 4 hearts per conditions ± s.e.m. **j**,**k**, Hearts were infused with vehicle or DMM before being retrieved from the thorax as previously described. Hearts were then exposed to 12 min WI, followed by 30 min CI, then 20 min WI to mimic the changes during anastomosis. Hearts were clamp frozen before measuring malonate (**j**) and succinate (**k**) levels by LC–MS/MS (data are mean ± s.e.m., $n = 3$; $^*P < 0.05$, $^{**}P < 0.001$ by a two-tailed Student's unpaired t-test).

nature research

Corresponding author(s): Michael P Murphy

Last updated by author(s): Mar 15, 2019

Reporting Summary

Nature Research wishes to improve the reproducibility of the work that we publish. This form provides structure for consistency and transparency in reporting. For further information on Nature Research policies, see Authors & Referees and the Editorial Policy Checklist.

Statistics

For all statistical analyses, confirm that the following items are present in the figure legend, table legend, main text, or Methods section.

n/a	Confirmed	
☐	☒	The exact sample size (*n*) for each experimental group/condition, given as a discrete number and unit of measurement
☒	☐	A statement on whether measurements were taken from distinct samples or whether the same sample was measured repeatedly
☐	☒	The statistical test(s) used AND whether they are one- or two-sided *Only common tests should be described solely by name; describe more complex techniques in the Methods section.*
☒	☐	A description of all covariates tested
☐	☒	A description of any assumptions or corrections, such as tests of normality and adjustment for multiple comparisons
☐	☒	A full description of the statistical parameters including central tendency (e.g. means) or other basic estimates (e.g. regression coefficient) AND variation (e.g. standard deviation) or associated estimates of uncertainty (e.g. confidence intervals)
☐	☒	For null hypothesis testing, the test statistic (e.g. *F*, *t*, *r*) with confidence intervals, effect sizes, degrees of freedom and *P* value noted *Give P values as exact values whenever suitable.*
☒	☐	For Bayesian analysis, information on the choice of priors and Markov chain Monte Carlo settings
☒	☐	For hierarchical and complex designs, identification of the appropriate level for tests and full reporting of outcomes
☒	☐	Estimates of effect sizes (e.g. Cohen's *d*, Pearson's *r*), indicating how they were calculated

Our web collection on statistics for biologists contains articles on many of the points above.

Software and code

Policy information about availability of computer code

Data collection	Labsolutions software (Shimadzu, UK)
Data analysis	XCalibur Qual and and XCalibur Quan Browser software (Thermo Fisher Scientific) BIORAD Quantilife software (BIORAD, UK) 'limma' package of R (http://bioconductor.org/packages/release/bioc/html/limma.html)

For manuscripts utilizing custom algorithms or software that are central to the research but not yet described in published literature, software must be made available to editors/reviewers. We strongly encourage code deposition in a community repository (e.g. GitHub). See the Nature Research guidelines for submitting code & software for further information.

Data

Policy information about availability of data

All manuscripts must include a data availability statement. This statement should provide the following information, where applicable:

- Accession codes, unique identifiers, or web links for publicly available datasets
- A list of figures that have associated raw data
- A description of any restrictions on data availability

Nearly all data are reported in the manuscript and in the supplemental files. There are no restrictions on data availability. The only original data not in the manuscript is that associated with chemical syntheses and this has been deposited at http://dx.doi.org/10.5525/gla.researchdata.646. In addition the metabolomic data have been uploaded as study MTBLS1085 to MetaboLights (https://www.ebi.ac.uk/metabolights).

Field-specific reporting

Please select the one below that is the best fit for your research. If you are not sure, read the appropriate sections before making your selection.

☒ Life sciences ☐ Behavioural & social sciences ☐ Ecological, evolutionary & environmental sciences

For a reference copy of the document with all sections, see nature.com/documents/nr-reporting-summary-flat.pdf

Life sciences study design

All studies must disclose on these points even when the disclosure is negative.

Sample size	Pilot experiments, as well as previous work in our laboratories, were used to predict effect size and indicated n=4-8 per group to be sufficient to detect biologically and statistically significant results. No sample size calculations were performed.
Data exclusions	No data were excluded from the data set.
Replication	The data were repeated on multiple independent animals. All replicates are true biological (rather than technical) replicates. All replicatiosn were successful.
Randomization	Animals were randomly allocated to control or treatment groups.
Blinding	In most cases, detailed in the methods sections, samples were analysed by a blinded observer. It was not possible to apply blinding to the surgical intervention themselves due to the nature of the interventions and the skills required to carry them out.

Reporting for specific materials, systems and methods

We require information from authors about some types of materials, experimental systems and methods used in many studies. Here, indicate whether each material, system or method listed is relevant to your study. If you are not sure if a list item applies to your research, read the appropriate section before selecting a response.

Materials & experimental systems

n/a	Involved in the study
☒	☐ Antibodies
☐	☒ Eukaryotic cell lines
☒	☐ Palaeontology
☐	☒ Animals and other organisms
☐	☒ Human research participants
☒	☐ Clinical data

Methods

n/a	Involved in the study
☒	☐ ChIP-seq
☒	☐ Flow cytometry
☒	☐ MRI-based neuroimaging

Eukaryotic cell lines

Policy information about cell lines

Cell line source(s)	C2C12 mouse myoblasts from American Type Cultute Collection (ATCC) (Middlesex, UK).
Authentication	Cell line was authenticated as supplied by the commercial vendor. In addition, C2C12 myoblasts were periodically differentiated in to myotubes, in our lab and markers of differentiation identified by western blotting, confirming the identity of the C2C12 cells.
Mycoplasma contamination	Cell line tested negative for mycoplasma infection in routine tests in the Cambridge MBU tissue culture facility.
Commonly misidentified lines (See ICLAC register)	No commonly missidentified cell lines wer used.

Animals and other organisms

Policy information about studies involving animals; ARRIVE guidelines recommended for reporting animal research

Laboratory animals	C57BL/6 female mice were purchased from Charles River Laboratories. Mice were maintained in specific-pathogen-free animal facilities with ad libitum access to food and water. Large white male (Landrace) pigs (45-55 kg) were supplied by Envigo and were acclimatised for a minimum of 7 days prior to experiments, with ad libitum access to food and water.
Wild animals	This study did not involve wild animals

Field-collected samples	This study did not involve animals collected from the field
Ethics oversight	All animal experiments were approved by the UK Home Office under the Animals (Scientific Procedures) Act 1986. Mouse experiments were covered by project license PPL 80/2638 and P7720A3D6. Pig experiments were performed under the Home Office Project License held by Envigo.

Note that full information on the approval of the study protocol must also be provided in the manuscript.

Human research participants

Policy information about studies involving human research participants

Population characteristics	Heart biopsies were taken from deceased human DBD donors deemed unsuitable for cardiac transplantation aged 36-69 (Table S1). Informed consent for the use of the human tissue for this project was provided by the donors' families.
Recruitment	Heart biopsies were taken from deceased human DBD donors deemed unsuitable for cardiac transplantation aged 36-69 (Table S1). Informed consent for the use of the human tissue for this project was provided by the donors' families.
Ethics oversight	Ethical approval for the studies was obtained from NRES Committee East of England – Cambridge South (REC Reference 15/EE/0152).

Note that full information on the approval of the study protocol must also be provided in the manuscript.